Colloid Polym Sci 279:1183–1191 (2001)

ORIGINAL CONTRIBUTION

Y. Tatek
E. Pefferkorn

Structural and stability characteristics of agglomerated clusters

Received: 25 January 2001
Accepted: 16 May 2001

Y. Tatek · E. Pefferkorn (✉)
Institut Charles Sadron
6 rue Boussingault
67083 Strasbourg Cédex, France
e-mail: peffer@cerbere.u-strasbg.fr

Abstract We investigated the cohesion of agglomerates formed by sticking two fractal clusters, each cluster having been previously generated by particle aggregation on a 3D lattice. The degree of cohesion of an agglomerate of a given configuration was defined by the number of connections simultaneously established on the two stuck clusters. All the possible nonoverlapping configurations were investigated and the corresponding porosity and brittleness as well as the pore volume and connection frequencies were determined. The numerical study showed the greater internal cohesion of agglomerates issued from sticking of reaction-limited aggregation (RLA) clusters compared to that of diffusion-limited-aggregation (DLA) clusters. DLA and RLA agglomerates presented continuously decreasing pore volume frequency curves, the latter agglomerates being characterised by a greater frequency of large pores. Comparison with typical controlled fragmentation experiments showed the number of connections to be the prevailing factor in the cohesion of aggregates formed in aqueous suspensions under various conditions.

Key words Agglomeration of fractals · Powder cohesion · Powder brittleness · Powder porosity · Connectivity of powder agglomerates

Introduction

Dry powder agglomerates are universally employed in industrial, biomedical and pharmaceutical applications and wet and dispersed powder agglomerates are found in agricultural soils and aquatic environments. Their sizes vary from nanometres to millimetres. There are many difficulties associated with the characterisation of such agglomerates owing to their complex surface structure and volume porosity. Actually, powders are far from being compact spheres and merely resemble fractal grains. Different systems have been investigated recently and recent results concerning the morphology of fractal aggregates in polymeric composites show the effect of powder dispersing mechanisms [1–3]. Taking this situation into account we attempted to determine the parameters which may characterise the agglomerate brittleness and the spatial distribution of voids within the agglomerate volume. Usually, agglomerate formation is mediated by additives, which means that the agglomerate cohesion is mediated by soft or hard adhesive bonds; thus, firm contacts between neighbouring particles belonging to stuck aggregates may not be required to build a stable structure. Obviously this situation may be schematised using on-lattice clusters as aggregate models. When no additives are added to powders and close contact between particles is required for cohesion, the situation may be better portrayed by employing off-lattice clusters to model the powder grain, but in the present study we also used on-lattice clusters to represent idealised real systems.

We first synthesised clusters which serve to model dispersed powder grains; thus, the fractal dimension of the clusters may be controlled and it will be later

possible to determine the influence exerted by the fractal dimension on the agglomerate characteristics. Actually, one may assume the spatial distribution of the particles within the cluster volume and the cluster compactness to exert strong influence on the brittleness and porosity of the agglomerates resulting from sticking. The second parameter concerns the masses of the clusters engaged in the agglomerate formation and their relative values, and it is, a priori, impossible to conjecture how that will influence these characteristics. Finally, the objective of the investigation was to extract the information mediated by the model, which may serve to deliver a qualitative valuable indication to obtained the characteristics of real systems, like agglomerates of carbon black and aerosils [4–10].

Characteristics of agglomerates issued from cluster sticking

Clusters serve to model the dispersed fractal powder grains; therefore, they constitute unbreakable constituents whose conformation cannot restructure in the present context [11]. Conversely, agglomerates are considered to be linked together by breakable connections in order to preserve some brittleness. Thus, the link established between stuck clusters, which may be characterised by the number, v, of connections which are concomitantly established, only refers to the connections which were established during the agglomerate formation. In the present model, the agglomerate mass is limited by the sticking of only two clusters.

Synthesis of the primary clusters

The possibility of simulating colloid aggregation using computers was recognised by Vold [12] and Sutherland [13], but large-scale numerical investigation became feasible only some years later. Simple computer models for cluster–cluster aggregation were used to study the structure of aggregates and the kinetics of their formation [14–16]. In the present diffusion-limited aggregation (DLA) [17], the 3D simulation is started by randomly occupying a small fraction (0.015) of the sites on the cubic lattice by particles. Initially, a particle is selected randomly and is moved by D lattice units, the direction of each of them being randomly chosen at each lattice site. Two particles stick when they share at least one face. This procedure is applied to all the particles. After this initial step, when clusters and particles are present on the lattice, at each time step, a particle or a cluster is selected randomly and is moved by the integer of $D/i^{0.5}$ lattice units, i being the mass of the cluster constituted of particles of mass 1. Different values of D were used as shown in Table 1.

When all the particles and clusters had moved once, a new run was started. When the first cluster of the required mass i is detected the simulation is stopped and the spatial coordinates of all the particles constituting that cluster are registered.

Since most of the real processes are more complex than the simple simulation of the DLA process described earlier, where all contacts between particles and/or clusters led to sticking, in a second set of simulations the algorithm was modified to take into account the effect of inefficient collisions on the aggregate structure [18]; therefore, the cluster mass-dependent mobility defined in the previous model was abandoned and the new condition (Eq. 1) was included in the algorithm in order to set the collision efficiency between clusters of masses i and j as mass dependent:

$$P_{ij} = P_0(ij)^{\sigma} \quad , \tag{1}$$

the values of P_0 and σ being reported in Table 1. As previously, the simulation run was stopped when the cluster of preselected mass i was obtained and the coordinates of all the particles constituting the cluster were registered.

These two algorithms for diffusion- and reaction-limited cluster–cluster aggregation were employed to generate 3D on-lattice clusters of masses ranging from 30 to 400. Since a simulation run only provided a single cluster, a great number of runs was performed in order to ensure that clusters of identical mass were characterised by various random conformations.

Synthesis of agglomerates

Computers were employed to determine the characteristics of all the spatial nonoverlapping configurations which may be formed by carrying out all the possible stickings of two clusters [19]. This was done systematically by testing the characteristics of all the configurations obtained by sticking when one cluster held at a

Table 1 Parameters of the diffusion-limited aggregation (*DLA*) and reaction-limited aggregation (*RLA*) processes

DLA	i	100	150	200	250	300	400
$D_i = D_1 i^{\gamma}$	D_1	10	13	14	16	18	20
	γ	−0.5	−0.5	−0.5	−0.5	−0.5	−0.5
RLA	i	50	100	150	200	300	
$P_{ij} = P_1(ij)^{\sigma}$	P_1	0.05	0.03	0.02	0.02	0.012	
	σ	0.4	0.4	0.4	0.4	0.4	

fixed position encounters a second mobile cluster. In contrast to the work reported in Ref. [19], the mobile cluster was rotated so that at the end of the process, the six facets of the mobile cluster have visited the six facets of the resting cluster and for each situation each facet of the mobile cluster was rotated four times to explore all the possible configurations of the ensemble of the two stuck clusters. Thus, each configuration corresponding to a given sticking was only counted once, but if an identical configuration was detected by chance, it was counted as an additional agglomerate since the same structure had a supplementary chance of being formed.

This detailed process was done using two clusters of different or equal masses and in the latter situation, the configuration of one cluster always differed from that of the other. Owing to the computation time required for carrying out the calculation on the numerous configurations, only ten "experiments" were performed for each set of agglomerate of given mass $(i + j)$ from sticking of clusters of mass i and j in order to get average characteristics.

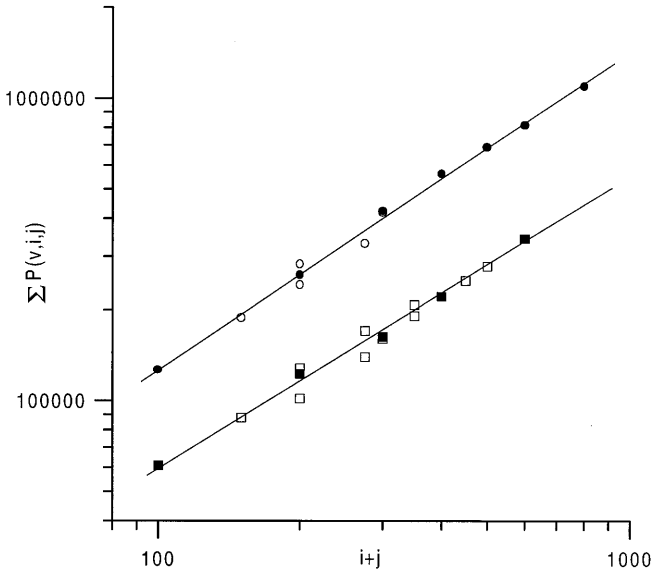

Fig. 1 Total number of nonoverlapping configurations obtained by all the possible assemblages of two clusters of similar (*filled symbols*) and dissimilar masses (*open symbols*) as a function of the mass $(i + j)$ of agglomerates constituted by clusters obtained by cluster–cluster diffusion-limited aggregation (●, ○) and cluster–cluster reaction-limited aggregation (■, □) processes

Results and discussion

The following characteristics of agglomerates formed by sticking clusters of mass i and j were determined:

- The connection frequency, $P(v, i, j)$.
- The total number of agglomerate configurations, $\sum P(v,i,j)$.
- The pore frequency, $c(s)$.
- The total porosity, V_1 and V_2.

Obviously, it was interesting to consider the possible correlation between these different characteristics and the agglomerate brittleness. The agglomerate brittleness is measured by the rate of aggregate fragmentation under given conditions.

Number of configurations

The total number, $\sum P(v,i,j)$, of nonoverlapping configurations resulting from the sticking of two clusters of identical masses i or different masses i and j as a function the total mass $(i + j)$ of the agglomerate is shown in Fig. 1. The number, v, of connections is determined by counting the number of common faces at the aggregate sticking limits as indicated in Fig. 2a, which shows a typical 2D configuration (for simplicity) obtained from the sticking of two identical 2D clusters of masses of 13, for which the number of connections is found to be 4. This configuration is identified under (4, 13, 13) and the frequency of the same configuration when all the possible configurations are analysed gives a value of $P(4, 13, 13)$.

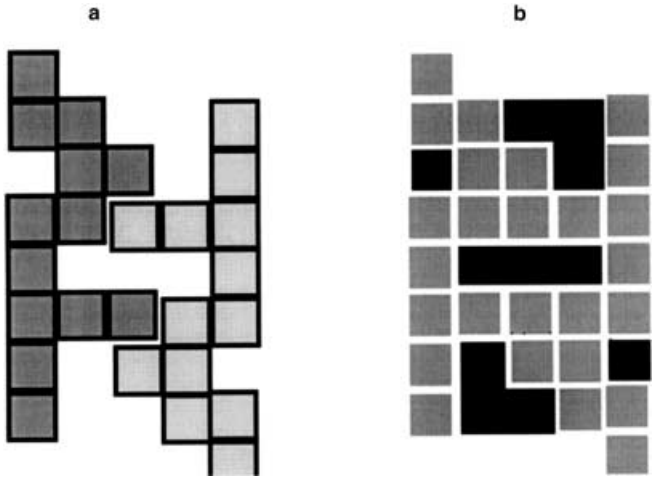

Fig. 2 a Representation of the assemblage of two 2D clusters developing a nonoverlapping configuration characterised by four connections. **b** In *black* the void of size $s = 11$ being affected by the agglomerate configuration

In Fig. 1, the lower and upper lines correspond to agglomerates obtained from the sticking of clusters generated by the algorithm of the reaction-limited-aggregation (RLA) and DLA processes, respectively. The following relationship is true for agglomerates of clusters of equal or unequal masses:

$$\sum P(v,i,j) \propto (i+j)^{v} \quad , \tag{2}$$

v being 1.04 and 0.93 for DLA and RLA systems, respectively.

For agglomerates of a given mass, the total number of agglomerate configurations, $\sum P(v,i,j)$, obtained for DLA systems is more than twice that obtained for RLA systems. DLA clusters offer two times more particles accessible to a mobile visiting cluster than RLA clusters. For a given type of clusters, the result shows that the number of complexion only depends on the total mass $(i + j)$ of the agglomerates and does not depend on the masses i and j of the individual stuck clusters. A small cluster i visiting the total periphery of a large cluster j produces the same number of configurations than two clusters of equal mass $(i + j)/2$ produce. Nevertheless, $\sum P(v,i,j)$ may be split into the product of two individual contributions, $\sum P(v,i)$ and $\sum P(v,j)$, the contribution of the cluster of mass i being given by Eq. (3):

$$\sum P(v,i) \propto i^{v/2} \quad . \tag{3}$$

Connection frequency

The number of connections concomitantly established when the agglomerate is formed was determined for each configuration resulting from the sticking of two clusters of masses i and j for $i = j$ or $i \neq j$. Then, the connection frequency, $P(v, i, j)$, was derived as a function of the connection number when all the $\sum P(v,i,j)$ had been analysed.

Two typical connection frequencies for agglomerates of mass (250 + 250) and (200 + 200) corresponding to sticking of clusters generated by DLA and RLA processes, respectively, are shown in Figs. 3 and 4. The value of the ordinate and the slope of variation of $P(v, i, j)$ versus v is a function of the agglomerate mass and of the type of cluster aggregation. The following relationship applies to the frequency of connections:

$$\log \frac{P(v,i,j)}{P(a,i,j)} = p(i,j) \times (1 - \vee) \quad , \tag{4}$$

where a is 1 for agglomerates of clusters generated by the DLA process and is very close to 1 for those generated by the RLA process. Obviously, the connection frequency decreases exponentially with the number of connections, and apparently the value of n does not exceed 20.

Brittleness of the agglomerate structure

It was interesting to determine the relative portion, $\Phi(m, i, j)$, (Eq. 5) of agglomerates for which clusters are linked together by m or more than m connections as a function of the agglomerate mass $(i + j)$ for $i = j$ and $i \neq j$.

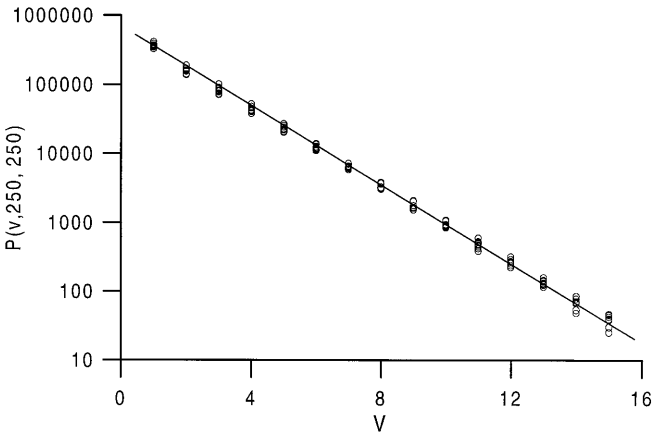

Fig. 3 Number of nonoverlapping configurations, $P(v, i, j)$, as a function of the number of connections, v, simultaneously established between two aggregates of equal masses of 250 obtained by cluster–cluster diffusion-limited aggregation

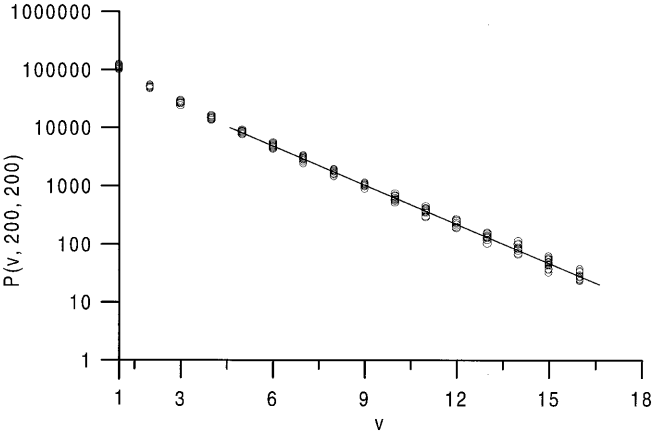

Fig. 4 Number of non overlapping configurations $P(v, i, j)$ as a function of the number v of connections simultaneously established between two aggregates of equal masses of 200 obtained by cluster–cluster reaction-limited aggregation

$$\Phi(m,i,j) = \frac{\sum\limits_{v \geq m} P(v,i,j)}{\sum\limits_{v} P(v,i,j)} \tag{5}$$

For very small agglomerates Eqs. (6) and (7) provide good fits of $\Phi(m, i, j)$ for stuck clusters generated by DLA and RLA processes, respectively:

$$\Phi(m,i,j) = \exp[0.693(1-m)] \quad , \tag{6}$$

$$\Phi(m,i,j) = 0.782 \exp[0.590(1-m)] \quad . \tag{7}$$

For agglomerates of intermediary masses, the contribution of the additional term $\delta[v(i + j)]$ cannot be ignored within the exponential term. For $(i + j) > 300$ plateau values of $\Phi(m, i, j)$ are obtained and the best fit corresponds to Eq. (8):

$$-\log \Phi(m) = km^{\alpha} \quad , \tag{8}$$

where k and α are 0.55 ± 0.01 and 1.03 or 0.39 ± 0.01 and 1.11 for agglomerated clusters formed by DLA or RLA processes, respectively. k is slightly mass dependent in the full range of $(i + j)$, while α is constant. Equation (8) strictly applies for $m > 3$, while a deviation appears for lower values as shown in Fig. 5.

Clearly, the relative portion of agglomerates linked by m connections is greater for agglomerated clusters generated by the RLA process than for those generated by the DLA process. Agglomeration of clusters generated by the DLA process should produce materials of greater brittleness than that of clusters generated by the RLA process if one assumes the correlation between brittleness and number of connections to be essential.

Agglomerate porosity

The voids within a cluster were determined to display the fractal character as was established in Refs. [20, 21]. In the present work, the porosity is defined by the number of voids within the agglomerate volume, the volume of each individual void being characterised by 1. As shown in Fig. 2b the void of size $s = 11$ includes the total internal volume and some external voids of very small volume, the filling of theses external voids requiring the formation of a great number of connections, which is statistically unfavourable (Figs. 6, 7); therefore, the void of volume s corresponds to the volume left vacant by s particles. The first result concerning the number of voids as a function the agglomerate mass $(i + j)$ is presented in Fig. 8. V_1 and V_2 correspond to the first and second moments of the pore volume frequency as defined by

$$V_f = \frac{\sum_s s^f n(s)}{\sum_v P(v, i, j)} \quad . \tag{9}$$

The following relationships between the voids V_1 and V_2 and the agglomerate mass $(i + j)$ were derived for agglomerated DLA or RLA clusters:

$$\text{DLA: } V_1 \propto (i+j)^{1.62} \quad V_2 \propto (i+j)^{2.20} \quad , \tag{10}$$

$$\text{RLA: } V_1 \propto (i+j)^{1.70} \quad V_2 \propto (i+j)^{2.88} \quad . \tag{11}$$

Clearly, the variation of V_1 with $(i + j)$ is quite similar for the two systems, whereas that of V_2 is different. The results shown in Fig. 8 indicate that the voids V_2 present within RLA agglomerates have larger volumes than those in DLA systems. Additionally, the exponents 2.88 and 2.20 show the portion of large volumes V_2 increase more strongly for RLA agglomerates than for DLA ones.

The variation of the porosity as a function of the total agglomerate volume is given by Eq. (12).

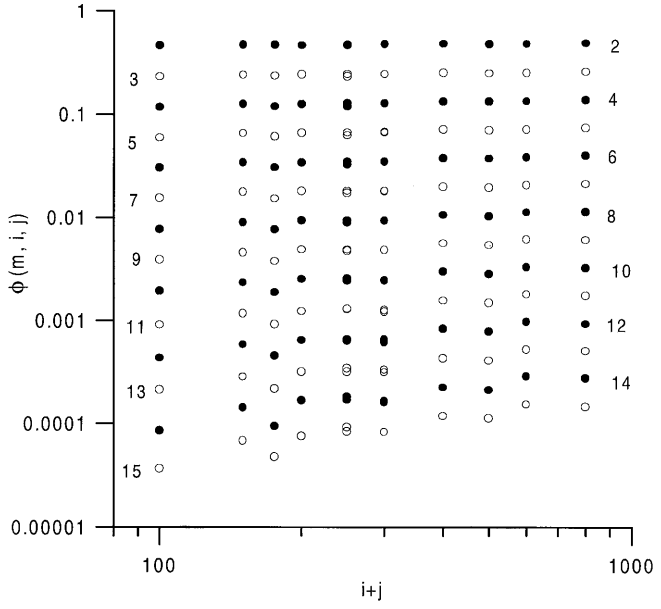

Fig. 5 Internal cohesion $\Phi(m, i, j)$ of agglomerates constituted by assemblages of aggregates of equal or unequal masses obtained by cluster–cluster diffusion-limited aggregation as a function of the agglomerate mass $(i+j)$. $\Phi(m, i, j)$ represents the portion of agglomerates connected by less than m interaggregate connections (the corresponding values of m are indicated on the curves)

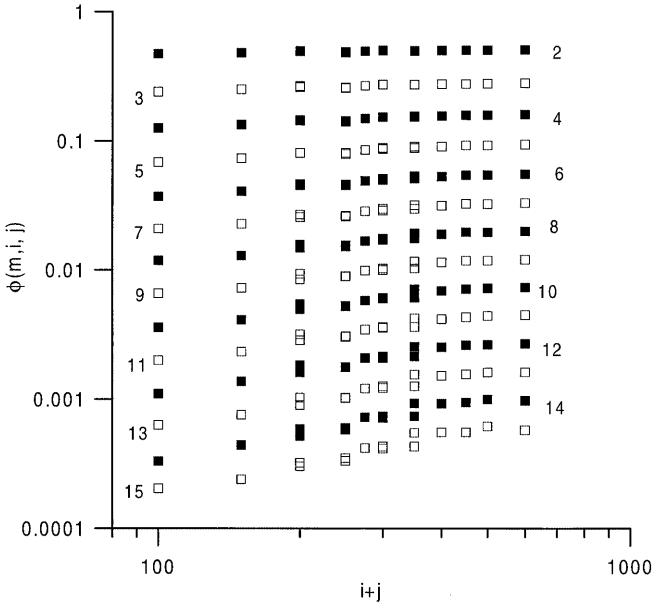

Fig. 6 Internal cohesion, $\Phi(m, i, j)$, of agglomerates constituted by assemblages of aggregates of equal or unequal masses obtained by cluster–cluster diffusion-limited aggregation as a function of the agglomerate mass $(i + j)$. $\Phi(m, i, j)$ represents the portion of agglomerates connected by fewer than m interaggregate connections (the corresponding values of m are indicated on the curves)

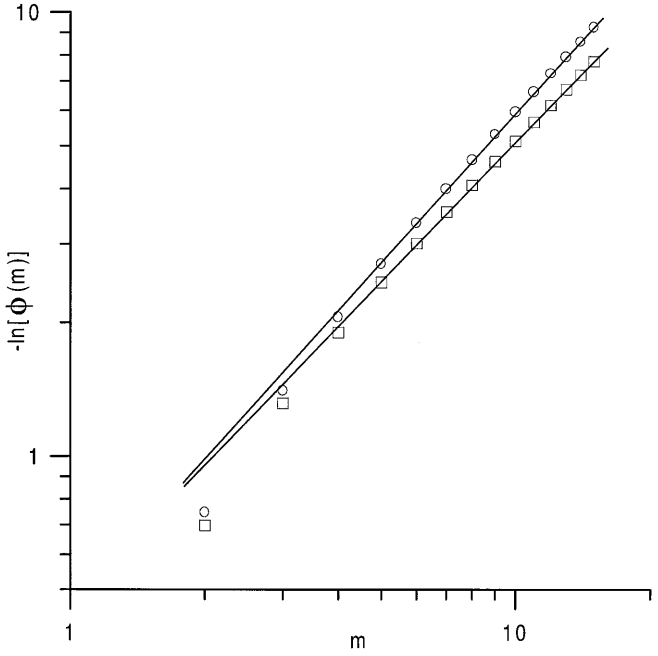

Fig. 7 Internal cohesion of agglomerates formed by assemblage of aggregates obtained by cluster–cluster diffusion-limited (○) and cluster–cluster reaction-limited aggregation (□) as a function of the number m of interaggregate connections being simultaneously established

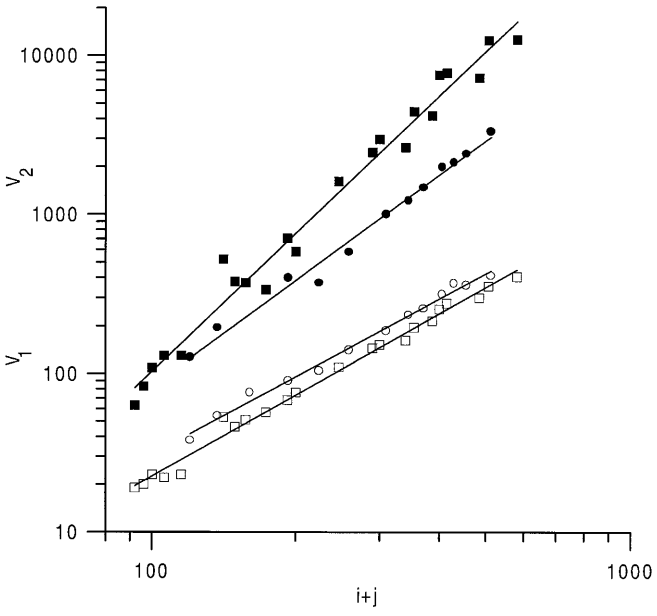

Fig. 8 Voids V_1 (*open symbols*) and V_2 (*filled symbols*) (Eq. 8) as a function of the agglomerate mass ($i + j$) for various agglomerates obtained by sticking of clusters generated by diffusion-limited aggregation (●, ○) and reaction-limited aggregation (■, □)

$$\text{Porosity} = \frac{V_1}{i+j+V_1} \propto \text{volume}^{\rho} \quad . \tag{12}$$

The exponent ρ was determined to be 0.33 and 0.44 for DLA and RLA systems, respectively. The porosity of DLA systems appears to be greater than that of RLA ones despite the fact that the porosity of the latter systems increases more strongly with the agglomerate mass ($i + j$), at least in the domain of masses explored.

Pore volume frequency

The pore volume frequency, $n(s)$, as a function of the pore volume, s, was calculated for DLA and RLA systems of different void volumes V_1 and V_2. The volume s was determined to vary between 1 and the maximum value of 100. Since pore fractals are simply the negative of mass fractals, Eq. (13) was used to show the self-similarity of the pore volume distribution as represented in Figs. 9 and 10 for DLA and RLA agglomerates, respectively.

$$n(s)V_2^2/V_1 \propto \left(\frac{s}{V_2}\right)^{-\eta} \quad . \tag{13}$$

From Eq. (13) values of η of 2.2 and 1.8 were derived for DLA and RLA systems. The monotonous decrease of the pore volume frequency indicates the presence of small voids at the maximum concentration, so the permeability of the system can only be ensured by connected voids of greater s values which are present at lower concentrations. In fact, the effective contribution of the various pores to the agglomerate porosity may be estimated by determining the variation of $s \times c(s)$ as a function of s. Actually, pores of volumes of $s = 20$ and 70 represent 1/100 of the volume attributed to pores of volume 1 for DLA and RLA agglomerates of masses of 500, respectively. Additionally, elements of size close to that of the particles which may be captured within voids at the moment of cluster sticking can remain isolated from the environment and can be liberated only by agglomerate breakup, and the conclusion may be similar for agglomerates of spherical particles.

Comparison with fragmentation experiments of latex aggregates suspended in aqueous solution

For a given m value $\Phi(m, i, j)$ decreases slightly with agglomerate mass and becomes constant for aggregates of mass greater than 300. The correlation between the brittleness of a given agglomerate configuration and the number of its interaggregate connections rests on the irregular fracture model of Horwatt et al. [22], for which the force binding the two clusters depends on the

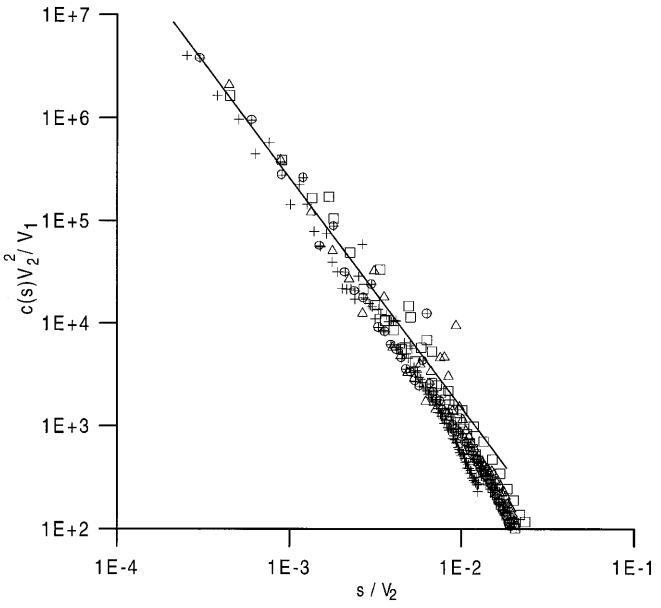

Fig. 9 Reduced void frequency as a function of the reduced void volume for agglomerates constituted by sticking of clusters generated by diffusion-limited aggregation processes. The different points correspond to agglomerates of different masses defined by their voids V_1 and V_2

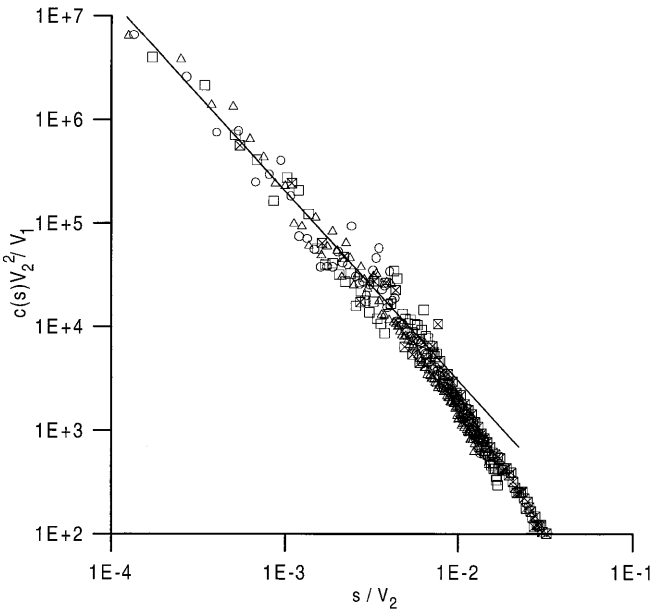

Fig. 10 Reduced void frequency as a function of the reduced void volume for agglomerates constituted by sticking of clusters generated by reaction-limited aggregation processes. The different points correspond to agglomerates of different masses defined by their voids V_1 and V_2

number of connections which must be severed in order to force the agglomerate to rupture. When shear was applied to determine the aggregate cohesion, Horwatt et al. found that the critical rupture stress decreased with increasing cluster size. The decrease is much more pronounced for the more tenuous DLA systems than for RLA ones. The authors concluded that additional parameters, such as an overall void fraction, the pore size distribution, or information on the connectivity is required for distinguishing the dispersion behaviour of various types of agglomerates.

We discuss the relative effect of these parameters on the rate of breakup of resting aggregates of latex particles sustaining controlled fragmentation in the absence of shear. One may effectively consider that the formation of aggregates of increasing mass results from agglomeration of two smaller clusters at each efficient collision and that all the possible configurations are realised for the growing system. It is very important to indicate that fragmentation did not progress randomly but that some "memory effects" led to preservation of the same reduced mass frequency during aggregation and fragmentation [23–25]. Therefore, fragmentation of a large aggregate (agglomerate) of mass $(i + j)$ corresponds to the separation of that agglomerate in the two aggregates of masses i and j which really did preexist during the aggregation step. The rate of fragmentation thus provides a good estimation of the agglomerate cohesion. Since these experimental results have already been published, only the experimental conditions and the main results are given to determine the leading parameters governing the agglomerate breakup taking into account the results obtained in this numerical study.

Aggregate fragmentation induced by rapid modification of the latex surface characteristics

Aggregation of latices of spherical shape and narrow size distribution (diameter of 1.3 μm) and bearing carboxylic acid groups (3 $\mu C/cm^2$) was induced by suspending the colloids in aqueous solutions of

- 0.15 mol/l NaCl at pH 2, 3 or 5 to induce the DLA process [24].
- 0.03 mol/l NaCl at pH 2, 3, 4 or 5 to induce the RLA process [25].

Periodically, aliquots of the aggregating suspensions were transferred to the fragmenting medium constituted by an aqueous solution of 1.5×10^{-4} mol/l NaCl at pH 7.0.

Increasing the pH and decreasing the ionic strength contributed to an increase in both the surface charge density and the range of the electrostatic forces. Owing to the high mobility of the proton, the modification of the latex surface characteristics was instantaneous. Because of the short time of 1–2 min required to determine the mass frequency curve of the fragments

employing a Coulter counter [26, 27], we concluded that the fragmentation observed was quite instantaneous.

Aggregate fragmentation induced by slow modification of the latex surface characteristics

Aggregation of latices of spherical shape and narrow size distribution (diameter of 0.885 μm) and bearing sulfonate surface groups (4.1 $\mu C/cm^2$) was induced by suspending the colloids in aqueous solutions of

- 1 mol/l NaCl at pH 3.0 to induce the DLA process [28].
- 0.15 mol/l NaCl at pH 3.0 to induce the RLA process [28].

Periodically, aliquots of the aggregating suspensions were transferred to the fragmenting medium constituted by an aqueous solution of poly(vinylpyridine) of molecular weight 5.89×10^5 at various high concentrations at the same pH of 3.0.

Immersion of the aggregates in the polyelectrolyte solution induces polymer adsorption on the latex surface, but the process was strongly delayed in time owing to surface exclusion and confinement effects resulting from the aggregate structure.

In these fragmentation experiments, the rate of variation of the agglomerate mass was slow and the agglomerate breakup rate, $a(i + j)$, was determined to be an increasing function of the agglomerate mass as expressed by Eq. (14) in agreement with earlier assumptions [29, 30] and recent theoretical results [31].

$$a(i+j) \propto (i+j)^{\lambda} \tag{14}$$

λ was derived from the cluster mass distribution curve $F(i + j)$ given using the particle counter. Cheng and Redner demonstrated that the rate of fragmentation, $a(i + j)$, of aggregates of size $(i + j)$ may be calculated from the variation of the cluster mass distribution in the range of the large masses [29, 30, 32]. λ derived from Eq. (15) was determined to be 0.6 and 0.5 for DLA and RLA systems, respectively. This small difference in the breakup rate can be attributed to the small difference in $\Phi(m)$ as indicated in Fig. 5.

$$F(i+j) = (i+j)^{-2}\exp\left[-\mathrm{a}(i+j)^{\lambda}\right] \tag{15}$$

Additionally, λ was determined to not depend on the polymer concentration in the fragmenting medium, but to decrease with the molecular weight of the polymer. Values of λ of 0.8, 0.6 and 0.4 were obtained for polymer of increasing molecular weight of 1.02×10^5, 5.89×10^5 and 1.057×10^6. This dependence indicates that the breakup results from the interfacial transfer of macromolecules from the solution to the confined surface area of the particles, the rate of the transfer decreasing with the molecular weight of the polymer.

Fragmentation of aggregates formed in the presence or in the absence of shear

Aggregation of latices of spherical shape and narrow size distribution (diameter of 1.73 μm) and bearing sulfonate surface groups (1.45 $\mu C/cm^2$) was induced by suspending the colloids in very dilute aqueous solutions of poly(vinylpyridine) of molecular weight 5.88×10^5 at pH 3.0. In the first set of experiments, the suspension was left to rest during aggregation carried out in a mixture of D_2O/H_2O to impede aggregate sedimentation (perikinetic aggregation), whereas in the second set, the suspension was continuously stirred (orthokinetic aggregation).

Periodically, aliquots of the aggregating suspensions were transferred to the fragmenting medium constituted by an aqueous solution of the same polymer at various higher concentrations at the same pH of 3.0 [33].

The fragmentation was thus induced by the progress of the polymer adsorption and as for aggregate fragmentation induced by slow modification of the latex surface characteristics, the rate of aggregate breakup obeys Eq. (14). Values of λ of 0.9 and 0.6 were determined to characterise the fragmentation rate of aggregates formed with and without stirring, respectively. The polymer concentration in the fragmenting medium and the degree of surface coverage established before the fragmentation was initiated were determined to not influence the rate of breakup. The difference in the breakup rates can be interpreted on the basis of the variation of $\Phi(m)$ with m. Therefore, since all the possible agglomerate configurations characterised by $1 < m < 20$ may be obtained when shear is not applied during aggregation, it may be assumed that with stirring agglomerate configurations linked by fewer than m connections do not survive shear stress and that only configurations with $m \leq v < 20$ are formed during orthokinetic aggregation. As a result, the connected areas are greater for agglomerates formed in the presence of shear than in the absence of shear.

Mechanism of the polymer-induced fragmentation

The diffusional mobility of the agent initiating the dispersion process should exert a great role since the fragmentation induced by the highly mobile Na^+ and H^+ ions was fast, whereas the fragmentation induced by the polymer adsorption was delayed in time and very slow. Taking into account the mass-dependent rate of breakup, which was determined when the fragmentation proceeds in polymer solutions [28], we conjectured that the agglomerate mean porosity may exert an additional influence on the rate of breakup. Actually, progressive dispersion of the agglomerated aggregates required that the polymer penetrate into the pores by diffusion and that polymer adsorption progress on freely available

surface areas as well as on facing confined areas. Breakup of a doublet requires the establishment of complete surface coverage on the two facing areas and breakup of an agglomerate into the two fragments requires the adsorption to be complete at the connected surface areas. The polymer accessibility to the confined surface areas is limited by the pore size distribution and pore connectivity within the agglomerates. The relatively greater values of $\Phi(m)$ determined for RLA systems ensure that the total confined surface area is greater for RLA than for DLA systems, on average. On the other hand, since the values of V_1 are greater for DLA agglomerates than for RLA ones, one may conjecture that agglomerate penetration by polymer molecules is faster in the first case. For the same reasons, the average cohesion of latex/polymer aggregates should be greater for aggregates formed in the presence of shear, for which the breakup rate varies as $(i + j)^{0.6}$ than for aggregates formed in the absence of shear, for which the breakup rate varies as $(i + j)^{0.9}$. Therefore, high porosity and a small number of connections (or small connected areas) are expected to increase the kinetics of agglomerate breakup processes.

Conclusion

The difference between DLA and RLA clusters was the fractal dimension, which is 1.78 and 2.04, respectively. Interestingly, this difference in fractal dimension was assumed to limit the structural resistance of pyrogenic and precipitated silica during axial compaction, the latter sustaining internal breakup at high pressure [34]. The present numerical study provided additional information on the connectivity and porosity of agglomerates constituted by DLA or RLA clusters. Connection and pore volume distributions were determined to well characterise agglomerated DLA or RLA systems. Although no information was obtained on the agglomerate permeability, the permeability of RLA agglomerates may be greater than that of DLA systems owing to the relatively higher concentration of pores of large volumes.

The use of macromolecules as dispersing agents and the determination of the rate of breakup in controlled fragmentation experiments allowed the cohesion of DLA and RLA aggregates of latex particles to be compared as well as that of aggregates formed in the presence and in the absence of shear, providing the molecular weight of the polymer and the other experimental conditions were held constant. Comparison with experiment confirmed the prevailing role of the number of internal connections in the agglomerate cohesion. It is thus obvious that the additive dose in powder agglomeration, which was considered to be optimal in the present simulation, should be crucial for optimisation of the additive mediated cohesion of powder agglomerates [35, 36].

Acknowledgement S. Stoll is acknowledged for providing the software employed to generate DLA and RLA clusters and for stimulating discussions.

References

1. Rieker TP, Hindermann-Bischoff M, Ehrburger-Dolle F (2000) Langmuir 16:5588
2. Carmona F (1988) Ann Chim 13:395
3. Rieker T, Misono S, Ehrburger-Dolle F (1999) 15:914
4. Bourrat X, Oberlin A, Van Damme H, Gateau C, Bachelar R (1988) Carbon 26:100
5. Ehrburger F, Tencé M (1990) Carbon 28:448
6. Salomé L, Carmona F (1991) Carbona 29:599
7. Li Q, Manas-Zloczower I, Feke DL (1996) Rubber Chem Technol 69:8
8. Starchev K, Petkanchin I, Stoylov S (1994) Langmuir 10:1456
9. Martin JE, Wilcoxon JP, Schaefer D, Odinek J (1990) Phys Rev A 41:4379
10. Hurd AJ, Flower WL (1988) J Colloid Interface Sci 122:178
11. Hess WM, Herd C (1993) In: Donnet JB, Bansal R, Wang MJ (eds) Carbon black. Dekker, New York, p 89
12. Vold M (1963) J Colloid Sci 18:684
13. Sutherland J (1967) J Colloid Interface Sci 25:373
14. Family F, Landau (eds) (1984) Kinetics of aggregation and gelation. Elsevier, Amsterdam
15. Jullien R, Botet R (1987) Aggregation and fractal aggregates. World Scientific, Singapore
16. Vicsek T (1989) Fractal growth phenomena. World Scientific, Singapore
17. Meakin P, Vicsek T, Family F (1985) Phys Rev B 31:564
18. Family F, Meakin P, Vicsek T (1985) J Chem Phys 83:4144
19. Jullien R, Kolb M (1984) J Phys A Math Gen 17:L639
20. Ehrburger F, Jullien R (1988) In: Unger KK (ed) Characterisation of porous Solids. Elsevier, Amsterdam, pp 441–449
21. Ehrburger-Dolle F, Mors PM, Jullien R (1991) J Colloid Interface Sci 147:192
22. Horwatt SW, Feke DL, Manas-Zloczower I (1992) Powder Technol 72:113
23. Stoll S, Pefferkorn E (1992) CR Acad Sci Paris Ser II 37
24. Stoll S, Pefferkorn E (1992) J Colloid Interface Sci 152:247
25. Stoll S, Pefferkorn E (1992) J Colloid Interface Sci 152:257
26. Pefferkorn E, Varoqui R (1989) J Chem Phys 91:5679
27. Walker PH, Hutka J (1971) Division of Soil Science. Technical paper 1:3
28. Ouali L, Pefferkorn E (1994) J Colloid Interface Sci 168:315
29. Cheng Z, Redner S (1988) Phys Rev Lett 60:2450
30. Cheng Z, Redner S (1990) J Phys A Math Gen 23:1233
31. Cheon M, Chang I (1999) Europhys Lett 46:6
32. Pefferkorn E (2001) In: Radeva T (ed) Physical chemistry of polyelectrolytes Surfactant science series. Dekker, New York, pp 509–566
33. Ouali L, Pefferkorn E (1994) J Colloid Interface Sci 161:237
34. Ehrburger F, Lahaye J (1989) J Phys (Paris) 50:1349
35. Tatek Y, Stoll S, Pefferkorn E (2001) Powder Technol 115:226
36. Yamada H, Manas-Zloczower I, Feke DL (1998) Rubber Chem Technol 71:1